2021 43rd Annual International Conference of the
IEEE Engineering in Medicine & Biology Society (EMBC)
Oct 31 - Nov 4, 2021. Virtual Conference

2021 43rd Annual International Conference of the IEEE Engineering in Medicine & Biology Society (EMBC) | 978-1-7281-1179-7/21/$31.00 ©2021 IEEE | DOI: 10.1109/EMBC46164.2021.9629890

Global Sensitivity Analysis For Clinically Validated 1D Models of Fractional Flow Reserve

Cyrus Tanade[1], Bradley Feiger[1], Madhurima Vardhan[1], S. James Chen[2], Jane A. Leopold[3], & Amanda Randles[1]

***Abstract*— Computation of Fractional Flow Reserve (FFR) through computational fluid dynamics (CFD) is used to guide intervention and often uses a number of clinically-derived metrics, but these patient-specific data could be costly and difficult to obtain. Understanding which parameters can be approximated from population averages and which parameters need to be patient-specific is important and remains largely unexplored. In this study, we performed a global sensitivity study on two 1D models of FFR to identify the most influential patient parameters. Our results indicated that vessel compliance, cardiac cycle period, flow rate, density, viscosity, and elastic modulus contributed minimally to the variance in FFR and may be approximated from population averages. On the other hand, outlet resistance (i.e., microvascular resistance), stenosis degree, and percent stenosis length contributed the most to FFR computation and needed to be tuned to the patient of interest. Selective measuring of patient-specific parameters may significantly reduce costs and streamline the simulation pipeline without reducing accuracy.**

I. Introduction

Fractional Flow Reserve (FFR) is a hemodynamic metric used to evaluate the functional significance of coronary atherosclerosis lesions. The standard-of-care is to take pressure measurements using a flow catheter, but this method is used in the minority of cases because it is costly and invasive [1]. To this end, several computational fluid dynamics (CFD) models [1], [2] have been developed to compute FFR. CFD is a branch of fluid mechanics that uses numerical analysis to solve the equations of fluid flow, where three-dimensional (3D) CFD models use 3D computational domains and one-dimensional (1D) models use compliant tubes with a single axial dimension. 3D models are able to capture complex hemodynamic patterns, but 1D models are often preferred for allowing blood flow to be simulated in a fraction of the time. While 1D models have been validated against 3D models and *in vivo* measurements of FFR, it remains unclear which parameters contribute significantly to FFR computation. CFD simulations generally aim to incorporate as much patient-specific data as possible to guide model inputs [3], but obtaining patient-specific measurements can be costly and time-consuming. We hypothesized that much of the data contributes minimally to CFD output and may be approximated from population averages. Here, we performed a global sensitivity study on clinically validated 1D models to identify parameters that contribute minimally to FFR.

[1] Department of Biomedical Engineering, Duke University, Durham, NC
[2] Department of Medicine, University of Colorado, Aurora, CO
[3] Department of Medicine, Brigham and Women's Hospital, Boston, MA

Previous work focuses on optimizing 1D models, identifying the most important parameters for FFR computation, and exploring the need for a separate pressure loss term (stenosis model) to capture the impact of a stenosis. Blanco *et al.* [1] found that using a 1D model improved correlation with 3D results when a stenosis model was defined ($r = 0.95$ vs. 0.88) [1]. However, Boileau *et al.* [2] demonstrated that a pressure loss model was not required to capture the impact of the stenosis compared with a 3D FFR simulation. Therefore, the need for a separate stenosis model remains a controversial topic. Yin *et al.* [4] used 1D models to perform a parameter sensitivity analysis and demonstrated that resistance accounted for the largest source of error in FFR calculation. Conversely, Fossan et al. [3] found that resistance and inlet flow rate contributed most to the variance in FFR. However, it is unclear whether other hemodynamic (vessel compliance, cardiac cycle period, viscosity, density) and geometric parameters (stenosis geometry, elastic modulus) are important in computing FFR. In short, understanding which parameters contribute minimally to FFR remains largely unexplored.

We first validated two 1D CFD models against *in vivo* measurements of FFR ($FFR_{clinical}$). The models included a stenosis model with an additional pressure loss term (FFR_S) and a no stenosis model (FFR_{NS}) without that term. The stenoses were unaltered in the patient-specific geometries for both models. We performed a global sensitivity analysis to determine which input parameters are important for FFR computation. Understanding which parameters to measure from patient data (i.e., patient-specific) and which parameters to approximate (i.e., non-patient-specific) is important as it could streamline the simulation workflow. In short, we made the following contributions: (1) validation of 1D computed FFR with *in vivo* FFR in 10 patients; (2) determination if stenosis models are required for accurate 1D FFR computation by comparing a stenosis and no stenosis model; and (3) identification of input parameters that could be approximated from population averages. Our results demonstrated that a stenosis model may not be required and that most parameters may be approximated from population averages.

II. Methods

A. Patient sample

Retrospective and de-identified data were acquired for ten patients from Brigham and Women's Hospital. The study was approved by the Partners Institutional Review Board.

Authorized licensed use limited to: Duke University. Downloaded on July 17,2025 at 03:00:27 UTC from IEEE Xplore. Restrictions apply.

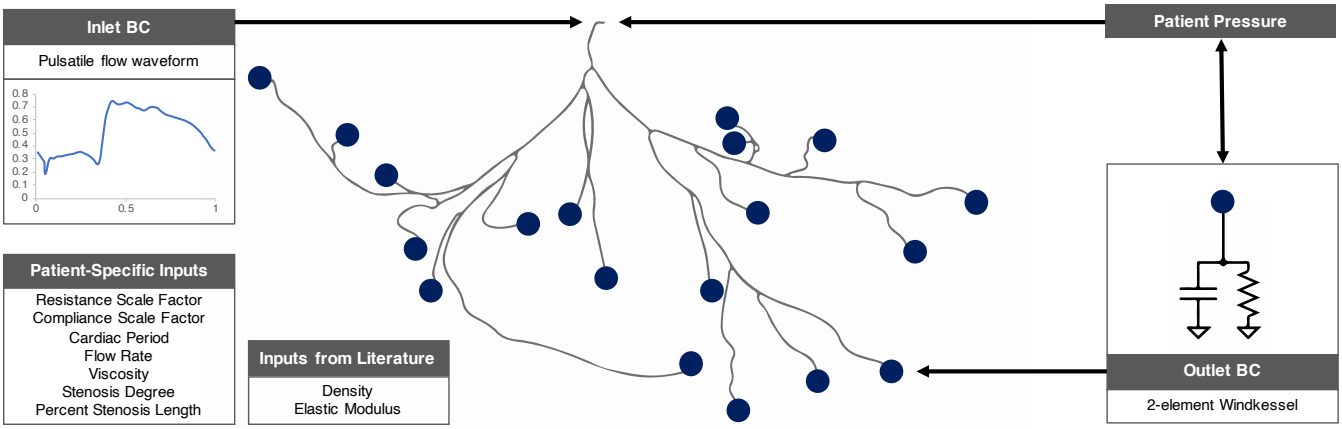

Fig. 1. **Boundary conditions and input parameters for 1D simulation.** Centerlines were used as the geometric input for 1D simulations. Pulsatile flow rate was used as the inlet boundary condition and a 2-element Windkessel (i.e., resistance and compliance) was used at the outlet boundary condition.

Imaging data were used to reconstruct geometries and extract stenosis degree and length. Cardiac cycle period, flow rate, and viscosity were derived from clinically measured hemodynamic data. *In vivo* FFR measurements were used as gold standard.

B. 1D modeling approach

3D coronary geometries were reconstructed from 2D angiograms using an algorithm that estimates cross-sectional diameters and centerlines. This methodology is described in Vardhan *et al.* [5], [6]. 1D coronary geometries were obtained by extracting the centerlines of 3D reconstructed geometries using Mimics (Materialise, Belgium). Stenosis degree and percent stenosis length were measured from 3D geometries using Blender (Blender Foundation, Netherlands).

We used a 1D blood flow simulator that is described in Feiger *et al.* [7]. The simulator was based on commonly used 1D blood flow equations derived from Navier-Stokes Equations (**Eqn.** 1) and was solved using a MacCormack finite difference scheme [7]:

$$\frac{\partial A}{\partial t}+\frac{\partial Q}{\partial x}=0,\ \frac{\partial Q}{\partial t}+\frac{\partial}{\partial x}\left(\alpha\frac{Q^2}{A}\right)+\frac{A}{\rho}\frac{\partial P}{\partial x}=-C_f\frac{Q}{A} \quad (1)$$

where A is cross-sectional area, Q is flow rate, P is pressure, ρ is density of blood, α describes the velocity profile, and C_f is a frictional term that incorporates dynamic viscosity. Furthermore, P is related to A (**Eqn.** 2):

$$P=P_{ext}+\beta(\sqrt{A}-\sqrt{A_0}),\ \beta=\frac{\sqrt{\pi}hE}{(1-\nu^2)A_0} \quad (2)$$

where P_{ext} is external pressure exerted on blood vessels and A_0 is the cross-sectional area when $P=P_{ext}$ [7]. β describes arterial stiffness and is a function of A_0, wall thickness (h), elastic modulus (E), and Poisson's ratio (ν). We used constant h of 0.945 mm [8] and E of 1.41 MPa [9] based on literature. ν was assumed to be 0.5 [10].

Blood was modeled as an incompressible Newtonian fluid with density of 1060 kg/m^3, and dynamic viscosity was derived on a per-patient basis using an experimentally derived relationship between hematocrit and viscosity described in [11]. To model the effects of the stenosis, we coupled the 1D model to a pressure loss term (**Eqn.** 3) for FFR_S:

$$\Delta P_s=\frac{\mu K_v}{2\pi r_u^3}Q+\frac{\rho K_t}{2A_u^2}\left(\frac{A_u}{A_s}-1\right)^2|Q|Q+\frac{\rho K_u L_s}{A_u}\frac{\partial Q}{\partial t} \quad (3)$$

where ΔP_s is pressure drop across a stenosis, μ is blood dynamic viscosity, r_u is radius of unstenosed artery, A_u is cross-sectional area of unstenosed artery, A_s is cross-sectional area of stenosed artery, and L_s is stenosis length. K_v, K_t, and K_u are viscous, turbulent, and inertial coefficients respectively, with $K_v=32(0.83L_s+1.64D_s)\times(A_u/A_s)^2/D_u$, $K_t=1.52$, and $K_u=1.2$. D_u and D_s are diameters that correspond to A_u and A_s, respectively.

Our boundary conditions incorporated a pulsatile flow waveform at the inlet, derived from clinically measured coronary fraction and waveforms in the literature [12], and 2-element Windkessel models at the outlets (**Fig.** 1). Outlet resistance-compliance values were computed using pressure measurements recorded from patient data and the expected flow rate at each outlet (**Fig.** 1). The expected outlet flow rates were estimated using Murray's Law [13]. We iteratively scaled resistance-compliance outlet values collectively until we matched clinically measured hyperemic systolic and diastolic pressure to a tolerance of 3%.

TABLE I
INPUT PARAMETER BOUNDS FOR 1D COMPUTED FFR

Parameter (Symbol)	Bounds	Unit
Outlet Resistance Scale Factor (R)	[0.760, 29.50]	-
Vessel Compliance Scale Factor (C)	[0.002, 0.060]	-
Cardiac Cycle Period (τ)	[0.566, 1.090]	s
Flow Rate (Q)	[1.64, 6.16]	cm^3/s
Density (ρ)	[1.02, 1.10]	g/cm^3
Viscosity (μ)	[1.70, 2.08]	cP
Elastic Modulus (E)	[1.19, 1.55]	MPa
Stenosis Degree (S_R)	[14.1, 52.1]	%
Percent Stenosis Length (S_L)	[8.50, 39.8]	%

C. Global sensitivity analysis

Parameters explored in the global sensitivity study (**Table** I) were assumed to be independent and to follow a uniform

Authorized licensed use limited to: Duke University. Downloaded on July 17,2025 at 03:00:27 UTC from IEEE Xplore. Restrictions apply.

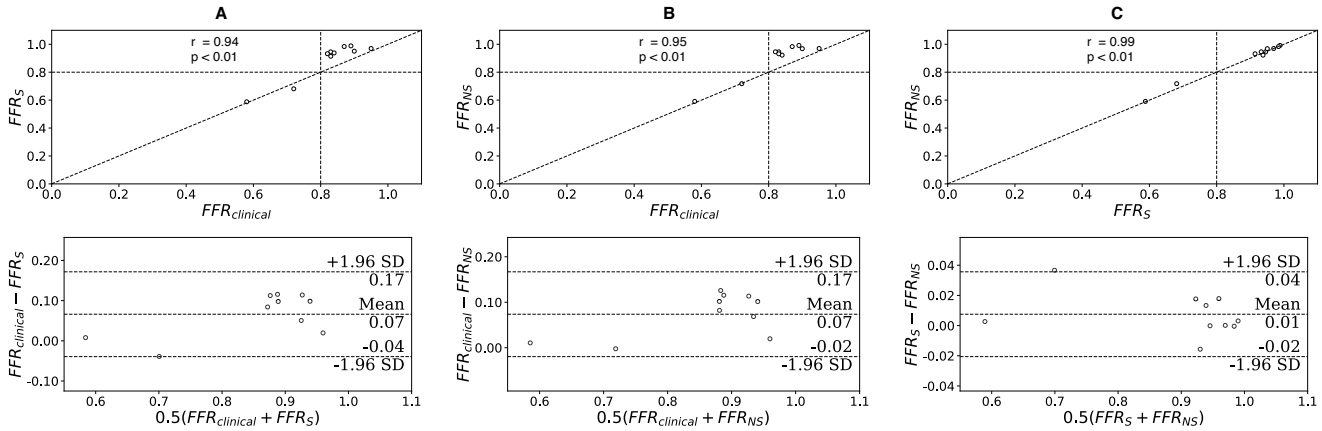

Fig. 2. **Correlation and agreement between 1D and *in vivo* FFR.** The columns compare (**A**) FFR_S and $FFR_{clinical}$, (**B**) FFR_{NS} and $FFR_{clinical}$, and (**C**) FFR_S and FFR_{NS}. Scatter plots (top row) demonstrated good correlation and Bland-Altman plots (bottom row) revealed bias in some cases.

distribution. Due to the variability of parameter bounds in the literature [3], [4], we obtained parameter bounds from our patient cohort. Outlet resistance (i.e., microvascular resistance), vessel compliance, density, and elastic modulus were not clinically measured but derived from literature or estimated. As resistance and compliance vary at each outlet for all geometries, we scaled resistances and compliances on a per-patient level to preserve flow distribution.

First-order (S_i) and total Sobol indices (S_{Ti}) were computed for each parameter based on the framework from Eck *et al.* [14] and averaged over all patients. We used a Monte Carlo approach to elucidate the contribution and interaction of input parameters on FFR. S_i quantifies the proportion that each parameter (Z_i) contributes to the total variance in FFR ($\mathbb{V}[Y]$) when neglecting interaction (**Eqn.** 4):

$$S_i = \frac{\mathbb{V}[\mathbb{E}[Y|Z_i]]}{\mathbb{V}[Y]} \tag{4}$$

where $\mathbb{V}[\mathbb{E}[Y|Z_i]]$ is the variance of the expected value of output Y given a fixed value of input parameter Z_i [14]. S_{Ti} quantifies the contribution to the total variance as well as all interaction effects for each parameter (**Eqn.** 5):

$$S_{Ti} = 1 - \frac{\mathbb{V}[\mathbb{E}[Y|Z_{-i}]]}{\mathbb{V}[Y]} \tag{5}$$

where Z_{-i} is a set of all input parameters excluding Z_i [14]. The second order Saltelli sequence was used over the Sobol sequence to minimize error rates in the Sobol indices. Convergence was assumed to occur when the bootstrapped 95% confidence interval width of each Sobol index was smaller than 10% of the maximum Sobol index for each parameter [15]. 2.4 million simulations were run on the Duke Compute Cluster to achieve converged Sobol indices.

III. Results

A. Clinical validation

FFR_S and FFR_{NS} both correlated well with $FFR_{clinical}$ ($r = 0.94$ and 0.95, respectively). The scatter plots in **Fig.** 2 demonstrated that there was a tendency for both 1D models to overestimate FFR for lesions with $FFR_{clinical} > 0.80$, but both models had better correlation for $FFR_{clinical} \leq 0.80$. These observations were also seen in the Bland-Altman plots in **Fig.** 2, where FFR_S and FFR_{NS} had bias of 0.066 ($CI : [0.028, 0.105]$) and 0.074 ($CI : [0.040, 0.108]$), respectively. Nevertheless, both 1D models correctly predicted if lesions were above or below 0.80 in all 10 patients.

When comparing FFR_S to FFR_{NS}, **Fig.** 2 demonstrated a near-perfect Pearson's correlation of 0.99, and the Bland-Altman plot in **Fig.** 2 indicated almost no bias between the two models (0.018, $CI : [-0.003, 0.018]$). Therefore, coupling the 1D model to a separate pressure loss term may not be required to compute FFR accurately.

B. Global sensitivity study

The global sensitivity study revealed that few parameters significantly contributed to the variance in FFR. S_{Ti} and S_i were similar, which suggests that interactions between parameters were negligible. **Fig.** 3 demonstrated that only outlet resistance (R) and stenosis degree (S_R) significantly contributed to variance for FFR_S, while only R significantly contributed to variance for FFR_{NS}. Without a stenosis model, S_R contributed less to the variance compared to simulations with a stenosis model. The relative contribution of R increased in simulations without a stenosis model. Since R was tuned against clinically measured pressure data, the results suggest that prescribing accurate outlet boundary conditions were essential for computing FFR.

Between FFR_S and FFR_{NS}, the sensitivity of the model to percent stenosis length (S_L) increased when neglecting the stenosis model. Given how close it was to the 0.05 sensitivity threshold [15], it is possible that S_L could cross the threshold in different coronary lesions and patient cohorts for FFR_{NS}. On the other hand, compliance, cardiac period, flow rate, density, viscosity, and elastic modulus were far below the threshold for both 1D models, which suggests that they are unlikely to cross the threshold in different patient cohorts.

Authorized licensed use limited to: Duke University. Downloaded on July 17,2025 at 03:00:27 UTC from IEEE Xplore. Restrictions apply.

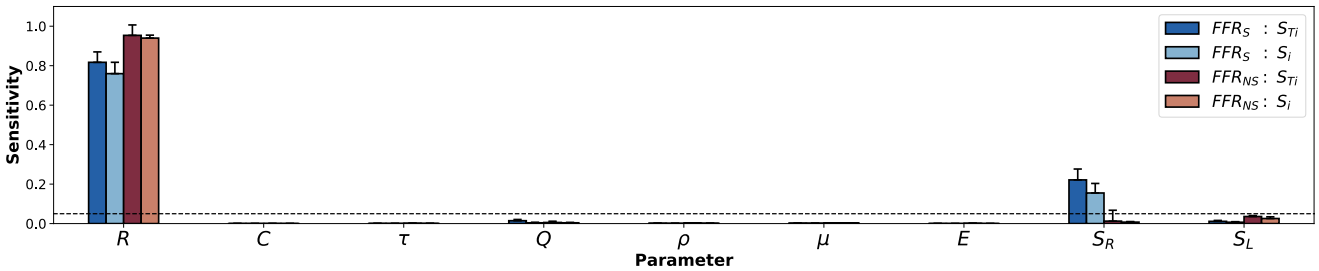

Fig. 3. **Global sensitivity analysis.** Sensitivity indices were averaged for all 10 patients. Error bars represent the standard error and the dotted line is the threshold for significance. Results demonstrate that the majority of parameters may be approximated from population averages.

IV. Discussion and Conclusion

Obtaining patient-specific parameters for CFD simulations is difficult and costly. Through sensitivity analysis, this work provided insight into which parameters could be approximated from population averages, and which parameters need to be patient-specific, for accurate FFR computation.

Comparing both 1D models to *in vivo* FFR revealed high correlation and agreement, and near-perfect correlation and agreement between both models. Global sensitivity analysis indicated that vessel compliance, cardiac cycle period, flow rate, density, viscosity, and elastic modulus do not significantly contribute to the variance in FFR and may be approximated from population averages, whereas only two parameters would need to be measured on a patient-specific level for FFR_S (R and S_R) and FFR_{NS} (R and S_L). R had the highest contribution to FFR, and this result is consistent with other global sensitivity studies [3], [4].

While FFR_S and FFR_{NS} were strongly correlated, the models differed based on the significant decrease in contribution of S_R. It was likely that FFR_{NS} was not able to effectively capture the full pressure drop when varying S_R to extreme values, but FFR_S was able to capture the full pressure loss as it directly modeled pressure loss across the stenosis and so had increased contribution to FFR.

This study had several limitations. There was a class imbalance between cases above and below 0.80. Based on our results, the 1D models computed FFR more accurately for cases below 0.80 than for cases above 0.80. The global sensitivity study was limited by the scope of the problem definition. Here, the majority of parameters considered were hemodynamic parameters, yet geometric parameters may also play an important role in computing FFR [16].

In conclusion, this work suggests that it is possible to prioritize several input parameters while approximating other parameters from population averages without trading-off performance. These findings could simplify parameter extraction workflow through reduced patient-specific data.

Acknowledgment

The authors thank Sayan Roychowdhury, Daniel Puleri, and Dr. Peter Balogh for feedback and discussions. Computing support for this work came from Duke OIT and the Duke Compute Cluster. This material is based upon work supported by the National Science Foundation Graduate Research Fellowship Program under Grant No. *NSF GRFP DGE 1644868*, NSF Grant 1943036, the AHA Predoctoral Fellowship Award No. 20PRE35211158, George Michael Memorial Fellowship and the NIH under Award Number U01CA253511. Any opinions, findings, and conclusions or recommendations expressed in this material are those of the author(s) and do not necessarily reflect the views of the NSF or the NIH.

References

[1] P. J. Blanco, C. A. Bulant, *et al.*, "Comparison of 1D and 3D Models for the Estimation of Fractional Flow Reserve," *Sci. Rep.*, 2018.

[2] E. Boileau, S. Pant, *et al.*, "Estimating the accuracy of a reduced-order model for the calculation of fractional flow reserve," *Int. J. Numer. Method. Biomed. Eng.*, 2018.

[3] F. E. Fossan, J. Sturdy, *et al.*, "Uncertainty Quantification and Sensitivity Analysis for Computational FFR Estimation in Stable Coronary Artery Disease," *Cardiovasc. Eng. Technol.*, 2018.

[4] M. Yin, A. Yazdani, and G. E. Karniadakis, "One-dimensional modeling of fractional flow reserve in coronary artery disease: Uncertainty quantification and Bayesian optimization," *Comput. Method. Appl. M.*, 2019.

[5] M. Vardhan, J. Gounley, *et al.*, "The importance of side branches in modeling 3D hemodynamics from angiograms for patients with coronary artery disease," *Sci. Rep.*, 2019.

[6] M. Vardhan, J. Gounley, *et al.*, "Non-invasive characterization of complex coronary lesions," *Sci. Rep.*, 2021.

[7] B. Feiger, A. Kochar, *et al.*, "Determining the impacts of venoarterial extracorporeal membrane oxygenation on cerebral oxygenation using a one-dimensional blood flow simulator," *J. Biomech.*, 2020.

[8] I. Gradus-Pizlo, S. G. Sawada, *et al.*, "Detection of subclinical coronary atherosclerosis using two-dimensional, high-resolution transthoracic echocardiography," *J. Am. Coll. Cardiol.*, 2001.

[9] A. Karimi, M. Navidbakhsh, *et al.*, "Measurement of the uniaxial mechanical properties of healthy and atherosclerotic human coronary arteries," *Mater. Sci. Eng., C.*, 2013.

[10] R. A. Baldewsing, C. L. de Korte, *et al.*, "A finite element model for performing intravascular ultrasound elastography of human atherosclerotic coronary arteries," *Ultrasound Med. Biol.*, 2004.

[11] B. Pirofsky, "The determination of blood viscosity in man by a method based on Poiseuille's law," *J. Clin. Investig.*, 1953.

[12] N. Hadjiloizou, J. E. Davies, *et al.*, "Differences in cardiac microcirculatory wave patterns between the proximal left mainstem and proximal right coronary artery," *Am. J. Physiol. Heart Circ.*, 2008.

[13] T. F. Sherman, "On connecting large vessels to small. The meaning of Murray's law.," *J. Gen. Physiol.*, 1981.

[14] V. G. Eck, W. P. Donders, *et al.*, "A guide to uncertainty quantification and sensitivity analysis for cardiovascular applications," *Int. J. Numer. Method. Biomed. Eng.*, 2016.

[15] N. Hsieh, B. Reisfeld, *et al.*, "Applying a Global Sensitivity Analysis Workflow to Improve the Computational Efficiencies in Physiologically-Based Pharmacokinetic Modeling," *Front. Pharmacol.*, 2018.

[16] L. Itu, S. Rapaka, *et al.*, "A machine-learning approach for computation of fractional flow reserve from coronary computed tomography," *J. Appl. Physiol.*, 2016.

Authorized licensed use limited to: Duke University. Downloaded on July 17,2025 at 03:00:27 UTC from IEEE Xplore. Restrictions apply.